Dynamical discontinuities in repeated weak measurements revealed by complex weak values

Lorena Ballesteros Ferraz[1]

[1] *Laboratoire de Physique Théorique et Modélisation (LPTM) – UMR CNRS 8089, CY Cergy Paris Université, Cergy-Pontoise, France*

(Dated: November 6, 2025)

Critical phenomena reveal universal behavior in complex systems, and uncovering analogous effects in quantum weak measurement protocols with post-selection provides new insight into how measurement backaction can shape quantum dynamics. This work investigates dynamical discontinuities that arise when the post-selected polar angle is used as a control parameter. The system evolves under repeated applications of a weak measurement protocol with post-selection, in which the meter state is retained after each iteration while the system is renewed. The emergence of these discontinuities is shown to be determined by the structure of the weak value: when the weak value has a nonzero imaginary component, a discontinuity appears in the expectation value of meter observables precisely at the point where the imaginary part of the weak value vanishes as a function of the post-selection polar angle. In contrast, no discontinuities occur when the weak value remains real for all post-selection angles. The phenomenon originates from the eigenstructure of the protocol's Kraus operator, with the stability of fixed points changing at the critical point where the discontinuity arises. Remarkably, the associated critical exponent is 1, independent of system parameters. These results open new perspectives for engineering non-analytic behavior in measurement-based quantum control and for probing criticality in post-selected quantum dynamics using weak measurements with weak values.

I. INTRODUCTION

Weak measurements with post-selection, first introduced by Aharonov and colleagues in [1], reveal a shift in the meter proportional to the so-called weak value, which can lie outside the eigenvalue spectrum of the measured observable. These anomalous weak values have proven useful both in foundational studies of quantum theory [2–7] and in enhancing sensitivity to weak signals in precision measurement and sensing applications [8–11]. Furthermore, weak values are closely connected to the Kirkwood–Dirac quasiprobability distribution, which exhibits nonclassical features whenever weak values are anomalous. In addition, anomalous weak values serve as evidence of contextuality in quantum mechanics [12–14].

The study of non-equilibrium quantum dynamics has revealed a rich landscape of critical phenomena that extend the concept of phase transitions beyond equilibrium physics. In addition to traditional equilibrium transitions driven by temperature or external fields [15–18], non-equilibrium settings exhibit sharp, non-analytic behavior in time-evolving observables [19, 20] and entanglement measures [21, 22]. Dynamical phase transitions, characterized by non-analyticities in quantities such as the Loschmidt echo following a quantum quench, have been widely explored in spin chains, cold-atom systems, and trapped-ion simulators, uncovering deep connections between dynamical criticality, equilibrium transitions, and excited-state quantum phase transitions [19, 23, 24].

In parallel, measurement-induced phase transitions have highlighted the fundamental competition between unitary entanglement generation and measurement-induced decoherence, leading to a transition between volume-law and area-law entangled phases in many-body systems [25–27]. These measurement-driven transitions exhibit universal scaling behavior reminiscent of classical percolation and have been observed in both numerical simulations and quantum experiments [28, 29]. Remarkably, signatures of criticality and non-analytic behavior are not restricted to the thermodynamic limit: even minimal systems, such as two-level and Rabi-type models, can display dynamical discontinuities when system parameters are tuned across critical regimes, suggesting that essential features of quantum criticality persist in few-body settings [30–32].

Although weak measurements with post-selection have been associated with mathematical features related to quantum criticality, such as non-normality [6], they have not yet been connected to critical phenomena, nor has the weak value been studied as a potential indicator of such behavior. This work investigates these aspects within a repeated weak measurement protocol.

This work investigates discontinuities, analogous to phase transitions, that emerge when the post-selection polar angle serves as the control parameter. Such discontinuities manifest in the expectation value of a meter observable after repeatedly applying the weak measurement protocol, as defined in [1], to the meter state. Analysis of the protocol's structure reveals the conditions under which discontinuities emerge. Importantly, my focus is not on the thermodynamic limit of many-body systems but rather on discontinuities within small systems. As a possible extension, one could explore whether enlarging the system Hilbert space enables genuine phase transitions in the thermodynamic sense.

The study examines how discontinuities emerge in the expectation value of meter observables during repeated weak measurement interactions. In each iteration, the system and meter interact via a weak unitary coupling, characterized by small interaction strength and short duration, after which the system is post-selected. The system is then discarded, while the meter is retained to interact with a new system initialized in the same initial state, following the same procedure. After N iterations, the expectation value of an observable (e.g., a Pauli operator $\hat{\sigma}$ for a two-level system) is evaluated as a function of the post-selection polar angle. Discontinuities arise precisely when the imaginary part of the weak value vanishes, provided that (i) the weak value is not purely real for all post-selection angles and (ii) the Kraus operator governing the meter's evolution has nondegenerate eigenvalues.

The study of quantum dynamics under repeated measurements has a long history, from the rigorous analyses of quantum nondemolition protocols [33, 34] to the exploration of measurement-induced phase transitions in many-body systems [35, 36]. In quantum nondemolition protocols and weak-measurement settings, repeated probe interactions lead to convergence toward stable fixed points or steady states, with convergence rates governed by the eigenstructure of the corresponding Kraus maps. However, these processes are typically continuous in their control parameters and do not exhibit sharp dynamical discontinuities. In contrast, many-body measurement-induced transitions [35] show non-analytic behavior in entanglement measures as a function of measurement strength, although the mechanism arises from competition between unitary and non-unitary dynamics. More recently, repeated weak measurements of non-conserved observables have been shown to yield partial collapse and emergent steady-state structures [37], but again without the appearance of discontinuous expectation values. This work differs by demonstrating that discontinuities can emerge even in a minimal two-particle setting, when the imaginary component of the weak value crosses zero, producing an exchange of stability bifurcation in the dynamics of the associated Kraus map.

Extending the phase-transition analogy, the relaxation dynamics reveal a critical exponent of 1, independent of system parameters, highlighting a form of universality. Nevertheless, it should be emphasized that these discontinuities do not constitute true phase transitions, as no thermodynamic limit is involved. However, by extending the meter dimension, one could potentially approach such a limit.

This paper is organized as follows: section II introduces the system and analyzes the Kraus operator associated with the protocol. Section III examines the fixed points of the protocol and their stability. Section IV specializes the discussion to the two-level case. Section V presents the analysis of the critical exponent associated with the observed discontinuities, and Section VI summarizes the main conclusions.

II. PROTOCOL PRESENTATION

This section introduces the protocol that gives rise to discontinuities and stability bifurcations, and examines the associated Kraus operator. Several qubits serve as the "systems" in a standard weak measurement protocol with post-selection, while an N-level system acts as the meter, the system in which discontinuities are induced. The system starts in the state $|\psi_S\rangle$, while the meter is initialized in the state $|\phi_A\rangle$. The joint initial state is

$$|\Psi\rangle = |\psi_S\rangle \otimes |\phi_A\rangle . \tag{1}$$

The system and meter interact weakly through a unitary operator $\hat{U}$ which, assuming the interaction strength g and the time t are sufficiently small, can be expanded to first order in g as

$$\hat{U} = e^{-igt\hat{O}_S\otimes\hat{O}_A} \approx \hat{I}\otimes\hat{I} - igt\,\hat{O}_S\otimes\hat{O}_A, \tag{2}$$

where $\hat{O}_S$ acts on the system and $\hat{O}_A$ on the meter.

After the interaction, the system is post-selected onto the state $|\psi_f\rangle$. The meter state $\hat{\rho}_A^f$ after applying once the weak measurement protocol is obtained via the application of the following Kraus operator $\hat{K}$ to the initial meter state:

$$\hat{\rho}_A^{f,1} = \frac{\hat{K}\,|\phi_A\rangle\,\langle\phi_A|\,\hat{K}^\dagger}{\mathrm{Tr}\Big[\hat{K}\,|\phi_A\rangle\,\langle\phi_A|\,\hat{K}^\dagger\Big]}, \tag{3}$$

where $\hat{K}$ is, in general, non-unitary and, to first order in g, can be expressed as

$$\hat{K} = \langle\psi_f|\psi_S\rangle\left[\hat{I} - igtO_{S,w}\hat{O}_A\right], \tag{4}$$

where

$$O_{S,w} = \frac{\langle\psi_f|\,\hat{O}_S\,|\psi_S\rangle}{\langle\psi_f|\psi_S\rangle} \tag{5}$$

is the weak value of the observable $\hat{O}_S$.

The Kraus operator remains non-unitary at first order in g as long as the imaginary part of the weak value is nonzero. To generate a dynamical process and observe discontinuities in the expectation value of certain observables in the meter's final state, the weak measurement protocol is applied n times, each involving a different system prepared in the same initial state, as illustrated in Fig. 1. Consequently, the meter state after the n applications is

$$\hat{\rho}_A^{f,n} = \frac{\hat{K}^n\,|\phi_A\rangle\,\langle\phi_A|\,\hat{K}^{\dagger!n}}{\mathrm{Tr}\Big[\hat{K}^n\,|\phi_A\rangle\,\langle\phi_A|\,\hat{K}^{\dagger!n}\Big]}, \tag{6}$$

where the Kraus operator $\hat{K}$ has been applied n times to the initial meter state.

The weak measurement protocol to reach the discontinuity (Fig. 1), consisting of pre-selection, a weak unitary interaction, and post-selection, is applied to the meter, with the entire process represented by the Kraus operator $\hat{K}$. After each full application of the weak measurement protocol, the system is discarded and replaced with a new one for the next iteration, while the meter is preserved throughout all n applications. The eigenvalues of

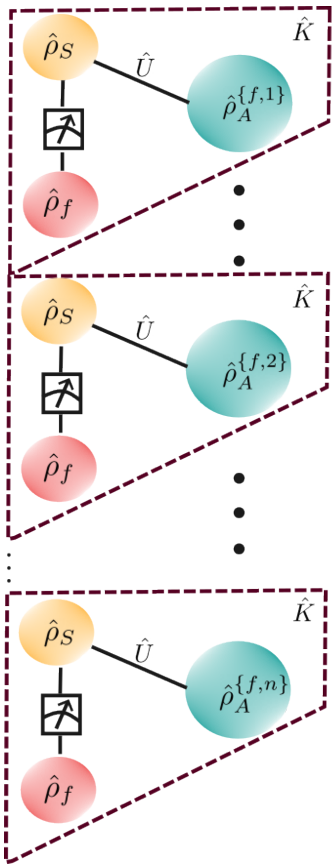

Figure 1. The protocol consists of the application of n times the weak measurement protocol where the system is pre-selected ($\hat{\rho}_S$), then it interacts with the meter (in the state $\hat{\rho}_A^{f,i}$) via a weak unitary operator and finally the system is post-selected ($\hat{\rho}_f$). After this protocol a new system is pre-selected ($\hat{\rho}_S$) and the protocol continues using the same meter.

the Kraus operator $\hat{K}$ are

$$\lambda_j = \langle\psi_f|\psi_S\rangle\left[1 - igtO_{S,w}o_{A,j}\right], \tag{7}$$

where j runs from 1 to N, with N denoting the dimension of the operator, and $o_{A,j}$ representing the eigenvalues of the N-level operator $\hat{O}_A$. To the first order in gt, their moduli are

$$|\lambda_j| = |\langle\psi_f|\psi_S\rangle|\sqrt{1 - 2gt\,\mathrm{Im}(O_{S,w})\,o_{A,j}}. \tag{8}$$

Thus, the moduli of the eigenvalues are equal, $|\lambda_j| = |\lambda_{j'}|$, whenever $\mathrm{Im}(O_{S,w}) = 0$, i.e., when the imaginary part of the weak value vanishes, or when the operator $\hat{O}_A$ is degenerate. If $\hat{O}_A$ is non-degenerate, a transition from non-unitary to unitary dynamics at first order in gt occurs at $\mathrm{Im}(O_{S,w}) = 0$. At the point where the absolute values of the eigenvalues become equal, discontinuities may appear in the expectation values of observables in the meter state after applying the weak measurement protocol n times. Such discontinuities emerge precisely at the points where the absolute values of the eigenvalues coincide (Appendix A).

This behavior emphasizes the essential role of complex weak values: discontinuities in the dynamics can arise only when $O_{S,w}$ possesses a nonzero imaginary component for some post-selected polar angle. Conversely, if the weak value is purely real, all N eigenvalues coincide for every value of ϕ (the post-selected polar angle), and no discontinuities occur since the eigenvalues remain equal.

III. FIXED POINTS AND THEIR STABILITY

Let us consider the Kraus operator $\hat{K}$ associated with the weak measurement protocol with post-selection applied to the meter state, as defined in Eq. 4. Under the assumption that the initial meter state is pure, the Kraus map ensures that the system evolves only within the manifold of pure states, which, for a two-level system, is geometrically represented by the surface of the Bloch sphere. When the dynamics consist of repeated applications of $\hat{K}$, the fixed points of the evolution, those states that remain invariant once reached, correspond to the eigenvectors of $\hat{K}$. These eigenvectors coincide with those of the observable $\hat{O}_A$, denoted by $|a_j\rangle$, and defined by

$$\hat{O}_A|a_j\rangle = \lambda_j|a_j\rangle, \qquad \lambda_j \in \mathbb{R}, \tag{9}$$

where j runs from 1 to N, the dimension of the Hilbert space of the operator $\hat{O}_A$, and λ_j are its eigenvalues.

To analyze the stability of the process, n successive applications of the Kraus operator $\hat{K}$ are considered. The initial meter state can be expressed in the eigenbasis of the observable $\hat{O}_A$ as

$$|\phi_A\rangle = \sum_j c_j^{(0)}\,|a_j\rangle\,, \tag{10}$$

where $c_j^{(0)}$ denotes the initial amplitude associated with the eigenstate $|a_j\rangle$.

After n iterations of the weak measurement protocol, corresponding to n normalized applications of the Kraus operator $\hat{K}$, the probability of finding the meter in the component state $|a_j\rangle$ evolves as

$$|c_j^{(n)}|^2 = \frac{|c_j^{(0)}|^2\,\left|1 + 2gt\,\mathrm{Im}(O_{S,w})\,\lambda_j\right|^{2n}}{\sum_k |c_k^{(0)}|^2\,\left|1 + 2gt\,\mathrm{Im}(O_{S,w})\,\lambda_k\right|^{2n}}, \tag{11}$$

where λ_j is the eigenvalue of $\hat{O}_A$ associated with $|a_j\rangle$, and $O_{S,w}$ denotes the weak value of the system observable.

The meter state after n applications is therefore

$$|\phi_A^{(n)}\rangle = \sum_j c_j^{(n)}\,|a_j\rangle\,, \tag{12}$$

with coefficients $c_j^{(n)}$ resulting from n successive normalized applications of the Kraus operator $\hat{K}$, the amplitudes $|c_j^{(n)}|$ of which are determined by Eq. 11.

As $n \to \infty$, the system approaches a long-time limit characterized by a stable fixed point, which is the state toward which all other states converge, except for those corresponding to unstable fixed points. This stable state is the eigenvector of the Kraus operator associated with the largest value of $|1+\alpha\lambda_j|$, assuming that the Kraus operator spectrum is non-degenerate. The remaining eigenvectors correspond to unstable fixed points.

Because gt is always positive, the sign of the imaginary part of the weak value $\mathrm{Im}\,(O_{S,w})$ determines which eigenvector becomes stable. Specifically:

- If $\mathrm{Im}(O_{S,w}) > 0$, the stable state is the eigenvector with the largest eigenvalue λ_+.
- If $\mathrm{Im}(O_{S,w}) < 0$, the stable state is the eigenvector with the smallest eigenvalue λ_-.

Consequently, a discontinuity in the dynamics arises when the stability of the fixed points changes. This occurs precisely when the imaginary part of the weak value $\mathrm{Im}(O_{S,w})$ crosses zero, defining a critical post-selected polar angle ϕ_c.

When the weak value has no imaginary part, $\mathrm{Im}(O_{S,w}) = 0$, the situation changes qualitatively. In this case, no eigenvalue is favored over the others, and the evolution becomes effectively unitary at first order in gt, leading only to phase accumulation.

IV. QUBIT-QUBIT EXAMPLE

Consider a concrete example where both the meter and the system are qubits (two-level systems), following the same weak measurement setup as before. The initial system state lies on the meridian with zero phase, as given in the equation below.

$$|\psi_S(\theta)\rangle = \cos\theta\,|0\rangle + \sin\theta\,|1\rangle\,, \tag{13}$$

whereas the post-selected state is an arbitrary qubit state

$$|\psi_f(\phi,\alpha)\rangle = \cos\phi\,|0\rangle + e^{i\alpha}\sin\phi\,|1\rangle\,. \tag{14}$$

The unitary interaction is defined as

$$\hat{U}(\gamma) = e^{-i\gamma t\hat{\sigma}_z\otimes\hat{\sigma}_x} = \cos\gamma t\left(\hat{I}\otimes\hat{I}\right) - i\sin\gamma t\,(\hat{\sigma}_z\otimes\hat{\sigma}_x) \tag{15}$$

that is valid for all interaction strengths. The Kraus operator becomes

$$\hat{K} = c(\gamma)\hat{I} + d(\gamma)\hat{\sigma}_x, \tag{16}$$

with

$$\begin{aligned} c(\gamma) &= \cos\gamma t\ \langle\psi_f|\psi_i\rangle \\ &= \cos\gamma t\ \left(\cos\theta\cos\phi + e^{-i\alpha}\sin\theta\sin\phi\right) \\ d(\gamma) &= -i\sin\gamma t\ \langle\psi_f|\psi_i\rangle\,\sigma_{z,w} \\ &= -i\sin\gamma t\ \left(e^{-i\alpha}\sin\theta\sin\phi - \cos\theta\cos\phi\right). \end{aligned} \tag{17}$$

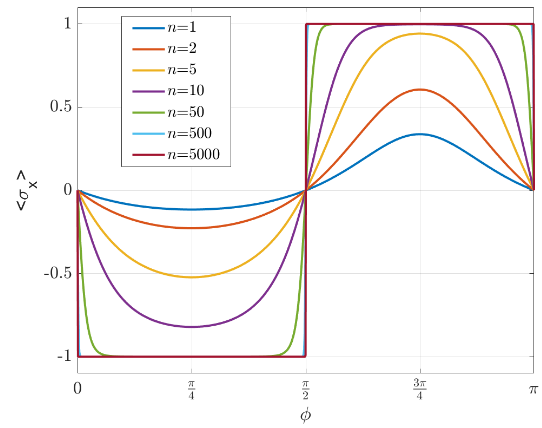

Figure 2. Three distinct discontinuities characterize the dependence of the expectation value of $\hat{\sigma}_x$ on the post-selected angle ϕ, emphasizing the nontrivial structure that arises for different repetition numbers n. In this plot $\alpha = \frac{\pi}{7}$, $\theta = \frac{\pi}{4}$ and $\gamma = 0.001$, while the initial meter state is along the z axis.

The corresponding eigenvalues are

$$\lambda_\pm = c(\gamma) \pm d(\gamma). \tag{18}$$

For a single repetition, the expectation value of the observable $\hat{\sigma}_x$ for the final meter state displays a smooth oscillatory behavior as a function of the post-selected polar angle (Fig. 2). As the number of repetitions of the protocol increases, however, the extrema become sharper, eventually forming a profile characterized by three distinct discontinuities. These discontinuities occur at the values of ϕ where the absolute values of the eigenvalues coincide, corresponding to the points where the imaginary part of the weak value vanishes, namely $\phi = 0$, $\phi = \frac{\pi}{2}$, and $\phi = \pi$. As predicted analytically, the eigenvalues have equal absolute values whenever the imaginary part of the weak value vanishes (Fig. 3).

Next, the discussion turns to the dynamics of the quantum state on the Bloch sphere, aiming to clarify how its trajectory relates to the observed discontinuous behavior. The trajectory of the state on the Bloch sphere can be expressed as

$$\begin{aligned} r_{x,n} &= \mathrm{Tr}\left[\hat{\sigma}_x\hat{\rho}_A^n\right] = \frac{a r_{x,n-1} + b + c}{a + (b+c)\,r_{x,n-1}} \\ r_{y,n} &= \mathrm{Tr}\left[\hat{\sigma}_y\hat{\rho}_A^n\right] = \frac{a r_{y,n-1} + i r_{z,n-1}\,(b-c)}{a + (b+c)\,r_{x,n-1}} \\ r_{z,n} &= \mathrm{Tr}\left[\hat{\sigma}_z\hat{\rho}_A^n\right] = \frac{a r_{z,n-1} - i r_{y,n-1}\,(b-c)}{a + (b+c)\,r_{x,n-1}}, \end{aligned} \tag{19}$$

where $a = |c\,(\gamma)\,|^2 + |d\,(\gamma)\,|^2$, $b = c\,(\gamma)\,d^*$, $c = c^*\,(\gamma)\,d\,(\gamma)$. Four distinct dynamical regimes emerge from the analysis. When the imaginary part of the weak value vanishes, the system exhibits purely unitary dynamics, resulting in periodic motion. In this case, the trajectories on the Bloch sphere are circular, with the initial parameter θ setting the starting point of the meter state (Fig. 4). This

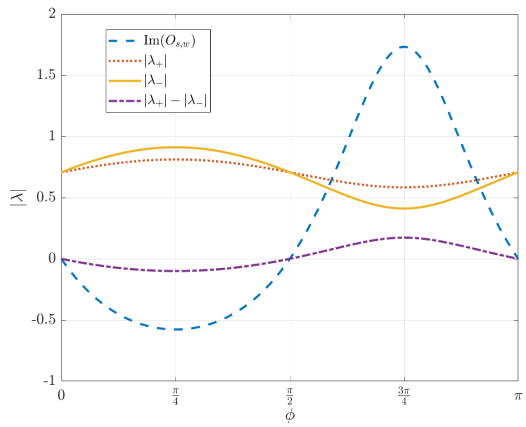

Figure 3. The imaginary part of the weak value vanishes when the absolute value of the two eigenvalues of the Kraus operator coincide. The plot shows the eigenvalues of the Kraus operator $\hat{K}$, $|\lambda_+|$ and $|\lambda_-|$, as functions of the post-selected angle ϕ, together with their difference $|\lambda_+|-|\lambda_-|$ and the imaginary part of the weak value $\mathrm{Im}(O_{s,w})$. In this plot $\alpha = \frac{\pi}{7}$, $\theta = \frac{\pi}{4}$ and $\gamma = 0.1$, while the initial meter state is along the z axis.

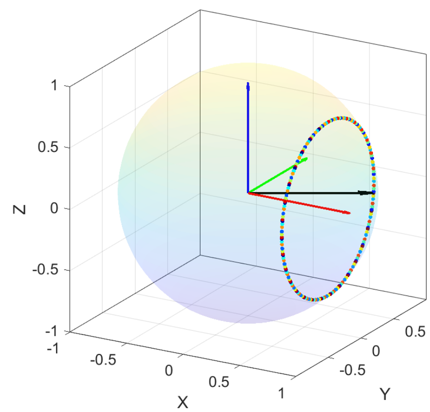

Figure 4. The Bloch sphere trajectory under unitary dynamics traces cycles at a constant polar angle, highlighting the periodic nature of the system. The path begins at the blue point and ends at the red point. System parameters are $\theta = \frac{\pi}{4}$, $\alpha = \frac{\pi}{7}$, $\gamma = 0.1$, $\phi = \frac{\pi}{2}$, with initial meter state $r = (\sqrt{0.5}, 0, \sqrt{0.5})^T$.

regime occurs for $\phi = 0$, $\frac{\pi}{2}$, and π, where the eigenvalues of the operator $\hat{K}$ coincide.

For values of ϕ such that $\phi \ll \frac{\pi}{2}$, two fixed points emerge, corresponding to the eigenvectors of $\hat{\sigma}_x$, the operator acting on the meter in Eq. 15. The fixed point at $x = -1$ is stable, while the one at $x = 1$ is unstable. Even if the state begins close to $x = 1$, the dynamics will eventually drive it toward the stable fixed point at $x = -1$ (Fig. 5). The dynamics will remain at $x = 1$ only when the system is initially exactly at that point. Conversely, for $\frac{\pi}{2} \ll \phi \ll \pi$, the stability of the fixed points is reversed: $x = 1$ becomes stable and $x = -1$ unstable. After passing $\phi = \frac{\pi}{2}$, the stable and unstable fixed points effectively swap roles. Finally, in the near-unitary regime, when the dynamics are close to but not exactly unitary, the trajectories cycle on the Bloch sphere before eventually collapsing onto the stable fixed point (Fig. 6).

It should be emphasized that the eigenvectors of the Kraus operator $\hat{K}$ remain constant and identical for all parameter values. Consequently, the point at which the stability of the fixed points changes cannot be characterized as an exceptional point, since the eigenvectors do not vary at that point.

V. ANALYSIS OF THE DISCONTINUITY

In second-order phase transitions, such as those in the Ising model [38] or the superconducting transition [39], the behavior of observables near the critical point is characterized by critical exponents that are universal across systems belonging to the same universality class. Typically, near the critical point of a control parameter P,

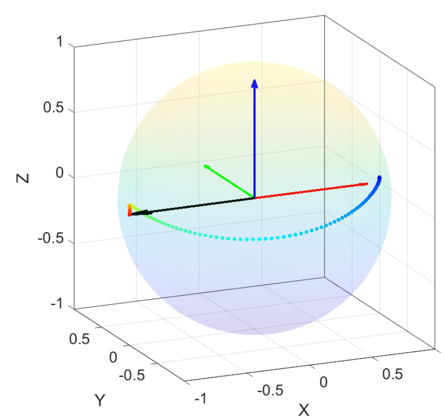

Figure 5. Although initiated near the unstable fixed point, the trajectory on the Bloch sphere is repelled toward the other fixed point, starting at the blue point and ending at the red point. Parameters: $\theta = \frac{\pi}{4}$, $\alpha = \frac{\pi}{7}$, $\gamma = 0.1$, $\phi = 1$, initial state $r = (\sqrt{0.99}, 0, \sqrt{0.001})^T$.

for instance, the temperature, the magnetic field, or the interaction strength in measurement-induced phase transitions [40], a characteristic physical quantity F (such as the heat capacity or the magnetic susceptibility) diverges following a power law in the vicinity of the critical point:

$$F(P) \propto |P - P_c|^{-\alpha}, \tag{20}$$

where P_c is the critical value of the control parameter and α is the associated critical exponent.

In the protocol studied in this article, the post-selected polar angle ϕ acts as the control parameter, governing a discontinuity in the expectation value of the Pauli matrix $\hat{\sigma}_x$ at the critical point ϕ_c. This discontinuity emerges af-

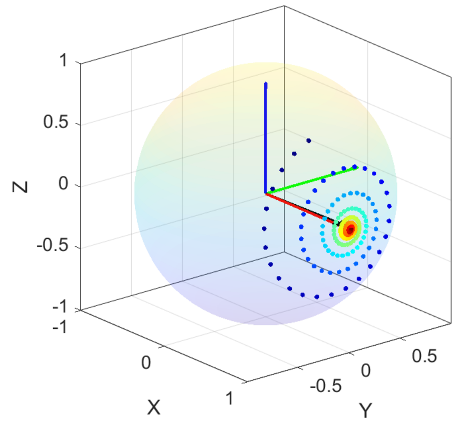

Figure 6. Starting near the unitary trajectory, the Bloch sphere path cycles while approaching the stable fixed point at $r=(1,0,0)^T$, beginning at the blue point and ending at the red point. Parameters: $\theta=\frac{\pi}{4}$, $\alpha=\frac{\pi}{7}$, $\gamma=0.1$, $\phi=\frac{\pi}{2}+0.1$, initial meter state $r=(\sqrt{0.5},0,\sqrt{0.5})^T$.

ter multiple iterations of the protocol. The corresponding relaxation time, defined as the time required for the system to reach its steady state, diverges at ϕ_c, since at the critical point the meter dynamics become effectively unitary and no single eigenstate (fixed point) dominates. Although the discontinuity observed in Fig. 2 might at first appear reminiscent of a first-order phase transition, the absence of a direct jump between two stable fixed points, and the emergence of unitary dynamics precisely at the critical point, indicate a resemblance to a second-order phase transition. The divergence of the relaxation time [41], demonstrated below, signifies critical slowing down, a defining feature of second-order phase transitions. Thus, the relaxation time τ serves as a key quantity for characterizing the critical behavior and determining the associated critical exponent, as well as for probing the universality of the transition. This section demonstrates that the relaxation time associated with the proposed protocol universally follows the power-law behavior expressed in:

$$\tau(\phi)\propto|\phi-\phi_c|^{-\nu}, \tag{21}$$

where ν is the critical exponent.
The precise definition of the relaxation time depends on the type of dynamics. Here, the dynamics proceed in discrete time steps, so τ can be defined in terms of the spectrum of the operator driving the dynamics, specifically the Kraus operator. This analysis determines the critical exponent from the relaxation dynamics, in analogy with dynamic Markovian processes [42, 43], where the key quantity is the ratio between the two leading eigenvalues of the Kraus operator. To quantify the convergence rate of the iterated Kraus map toward its fixed point, the relaxation time is defined in terms of the map's spectral properties. Consider the unnormalized meter state after n applications of the Kraus operator:

$$\rho_n^{(\mathrm{un})}=\hat{K}^n\rho_0\hat{K}^{\dagger n}=\sum_{i,j}\lambda_i^n\lambda_j^{*n}d_{ij}^0|\phi_i\rangle\langle\phi_j|, \tag{22}$$

where λ_i and $|\phi_i\rangle$ are the eigenvalues and eigenvectors of $\hat{K}$, and d_{ij}^0 are the coefficients of the initial meter density operator ρ_0.
Denoting by $|\lambda_1|$ and $|\lambda_2|$ the eigenvalues of the Kraus operator $\hat{K}$ with the largest moduli, such that $|\lambda_1|>|\lambda_2|$, the dominant diagonal term scales as $|\lambda_1|^{2n}$, while the next-to-leading term scales as $|\lambda_2|^{2n}$.
Consequently, the ratio between subdominant and dominant contributions decays as $(|\lambda_2|/|\lambda_1|)^{2n}$.
Matching this discrete decay to an effective exponential relaxation $e^{-n/\tau}$ defines the relaxation time τ:

$$\left(\frac{|\lambda_2|^2}{|\lambda_1|^2}\right)^n=e^{-n/\tau}\quad\Longrightarrow\quad\tau=\frac{1}{\log\left(\frac{|\lambda_1|^2}{|\lambda_2|^2}\right)}=\frac{1}{|\log R|}, \tag{23}$$

where $R=\frac{|\lambda_1|^2}{|\lambda_2|^2}$, and log denotes the natural logarithm. Near each discontinuity, when both moduli of the eigenvalues are equal, the relaxation time exhibits a divergence typical of dynamic critical phenomena. The study investigates whether this divergence follows a power-law behavior, as expressed in Eq. 21, considering the behavior both analytically, for any system governed by the protocol outlined in this article, and numerically, for the two-level system discussed in section IV.
For any system evolving under the dynamics dictated by the weak measurement protocol, the eigenvalues of the Kraus operator are given by Eq. 7. We assume that the meter operator $\hat{O}_A$ is non-degenerate. In this case, let us denote the largest eigenvalue in modulus by λ_1 and the second-largest by λ_2, corresponding to the eigenvalues o_1 and o_2 of the operator $\hat{O}_A$, respectively. The squared moduli of these eigenvalues can then be expressed, to first order in gt, as

$$|\lambda_{1,2}|^2\approx|\langle\psi_f|\psi_S\rangle|^2\left(1+2gto_{1,2}\mathrm{Im}\left(o_{S,w}\right)\right). \tag{24}$$

Consequently, the function R takes the form

$$R\approx\frac{\left(1+2gto_1\mathrm{Im}\left(o_{S,w}\right)\right)}{\left(1+2gto_2\mathrm{Im}\left(o_{S,w}\right)\right)}. \tag{25}$$

To calculate the critical exponent near the point where the imaginary part of the weak value vanishes, one can expand R in a Taylor series, assuming that $2gto_2\,\mathrm{Im}\left(o_{S,w}\right)$ and $2gto_1\,\mathrm{Im}\left(o_{S,w}\right)$ are small, and keeping terms to first order in gt as

$$\begin{aligned}R&\approx\left(1+2gto_1\mathrm{Im}\left(o_{S,w}\right)\right)\left(1-2gto_2\mathrm{Im}\left(o_{S,w}\right)\right)\\&\approx1+2gt\mathrm{Im}\left(o_{S,w}\right)\left(o_1-o_2\right).\end{aligned} \tag{26}$$

With this, the natural logarithm of R can be further expanded in a Taylor series as

$$\log\left(R\right)\approx2gt\mathrm{Im}\left(o_{S,w}\right)\left(o_1-o_2\right), \tag{27}$$

and, consequently, the relaxation time is given, to first order in gt, by

$$\tau \approx \frac{1}{|2gt\mathrm{Im}\,(o_{S,w})\,(o_1 - o_2)\,|}. \tag{28}$$

At $\phi = \phi_c$, the imaginary part of the weak value $\mathrm{Im}\,(o_{S,w})$, vanishes exactly. However, in typical cases of weak measurements, the weak value varies smoothly with the post-selected angle, so it is reasonable to assume that near ϕ_c, the imaginary part of the weak value depends linearly on ϕ as

$$\mathrm{Im}\,(o_{S,w}) \approx A|\phi - \phi_c|, \tag{29}$$

where A is a real constant. In this case, the relaxation time depends on ϕ according to

$$\tau \approx \frac{1}{|2gtA\,(\phi - \phi_c)\,(o_1 - o_2)\,|} \propto \frac{1}{|\phi - \phi_c|}, \tag{30}$$

which has the form of a power law, and by comparison with Eq. 21, one can deduce that the critical exponent is $\nu = 1$, independent of the meter dimension and other system parameters, provided the assumptions made in this section are satisfied.

To conclude this section, the qubit–qubit example of section IV serves to illustrate this behavior. Three divergences appear in the relaxation time τ as a function of the polar post-selection angle ϕ (Fig. 7). They correspond to the points where $\mathrm{Im}(O_{S,w}) = 0$ in the two-level system studied in section IV. At these points, the imaginary part of the weak value vanishes and the meter evolution becomes effectively unitary at first order in gt, coinciding with the discontinuities observed in the system's expectation values.

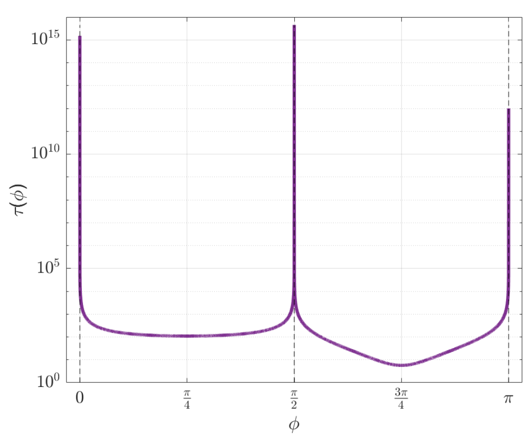

Figure 7. The relaxation time τ exhibits three divergences as a function of the polar post-selection angle ϕ at the critical points. The parameters used are $\alpha = \pi/7$, $\theta = \pi/4$, $\gamma = 0.01$.

The relaxation time τ near the three previously identified discontinuity points for the two-level system exhibits the expected power-law scaling, with linear fits giving a critical exponent of $\nu = 1$ (Fig. 8).

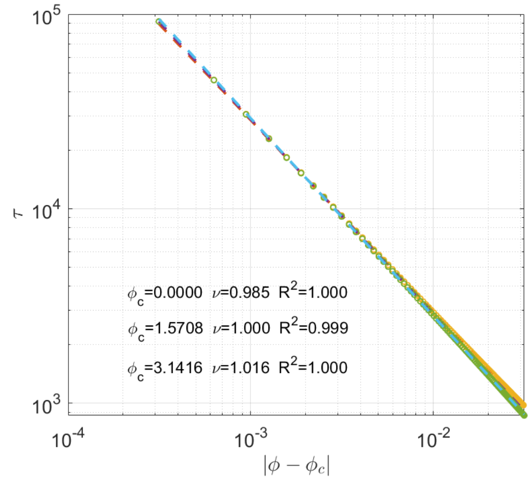

Figure 8. The relaxation time τ exhibits power-law scaling with exponent $\nu = 1$ near the three discontinuities, as shown in this log–log plot with linear regression fits. Parameters: $\alpha = \pi/7$, $\theta = \pi/4$, $\gamma = 0.01$.

VI. CONCLUSION

Complex weak values are essential for the emergence of such dynamical discontinuities, whereas purely real weak values suppress them. The relaxation time diverges at the critical point and exhibits a scaling law that appears to be universal, independent of the protocol parameters, with a critical exponent of 1. This behavior is reminiscent of second order phase transitions, as has been demonstrated analytically for systems of any dimension and confirmed numerically.

A nonzero imaginary part of the weak value modifies the system's evolution from a process that is unitary at first order in gt, where the Kraus operator has real eigenvalues of equal modulus at first order in gt, to a non-unitary dynamics featuring N fixed points, with N denoting the dimension of the system's Hilbert space. Among these, one fixed point is stable, provided that the Kraus operator is non-degenerate. In this case, the dynamics drives the system toward the stable fixed point, which corresponds to the eigenvector associated with the largest eigenvalue of the Kraus operator, unless the meter is initially prepared in exactly one of the other eigenvectors corresponding to unstable fixed points. This eigenvector coincides with the largest eigenvalue of the meter operator if the imaginary part of the weak value is positive, and with the smallest eigenvalue if the imaginary part of the weak value is negative.

Extending the detailed analysis to larger meter dimensions could reveal connections to genuine many-body phase transitions in the thermodynamic limit.

ACKNOWLEDGMENTS

I thank Alexandre Matzkin for fruitful discussions that enriched this work. I am grateful to Sébastien R. Mouchet for a careful reading of the manuscript and providing valuable suggestions. This research was supported by the EUTOPIA Science and Innovation Fellowship Programme and funded by the European Union Horizon 2020 programme under the Marie Skłodowska-Curie grant agreement No 945380.

Appendix A: Discontinuities from eigenvalue exchange

Discontinuities in the long-time meter state occur precisely when the eigenvalue of $K(\phi)$ with the largest modulus ceases to be dominant and another eigenvalue takes its place.
Let $\hat{K}(\phi)$ denote a family of linear operators on the finite-dimensional Hilbert space of the meter, representing the Kraus operators determined by the parameters of the protocol. This family depends continuously on the real parameter ϕ, the post-selected polar angle. The unnormalized map is

$$\hat{\rho}_{A,n}^{(\mathrm{un})}(\phi) = \hat{K}(\phi)^n \hat{\rho}_{A,0} \hat{K}(\phi)^{\dagger n}, \tag{A1}$$

for an arbitrary initial meter state $\hat{\rho}_{A,0}$. The normalized state after n iterations is

$$\hat{\rho}_{A,n}(\phi) = \frac{\hat{\rho}_{A,n}^{(\mathrm{un})}(\phi)}{\mathrm{Tr}[\hat{\rho}_{A,n}^{(\mathrm{un})}(\phi)]}. \tag{A2}$$

Assume that, for each ϕ, the operator $\hat{K}(\phi)$ is diagonalizable with eigenvalues $\{\lambda_j(\phi)\}$ and orthogonal eigenvectors $|\lambda_j(\phi)\rangle$, satisfying $\langle\lambda_i(\phi)|\lambda_j(\phi)\rangle = \delta_{ij}$. This assumption holds in the protocol, as the Kraus operators involve only the identity and an observable of the meter. This study focuses on non-degenerate observables.
Consider that, for $\phi < \phi_c$, the eigenvalue of $\hat{K}(\phi)$ with the largest modulus is unique and given by $\lambda_1(\phi)$, while for $\phi > \phi_c$ it is $\lambda_2(\phi)$, with

$$|\lambda_1(\phi_c)| = |\lambda_2(\phi_c)|. \tag{A3}$$

Let the corresponding normalized projectors be

$$\hat{P}^1 = \lim_{\phi\to\phi_c^-} \frac{|\lambda_1(\phi)\rangle\langle\lambda_1(\phi)|}{\langle\lambda_1(\phi)|\lambda_1(\phi)\rangle} \neq \lim_{\phi\to\phi_c^+} \frac{|\lambda_2(\phi)\rangle\langle\lambda_2(\phi)|}{\langle\lambda_2(\phi)|\lambda_2(\phi)\rangle} = \hat{P}^2, \tag{A4}$$

and assume $\langle\lambda_j(\phi)|\hat{\rho}_{A,0}|\lambda_j(\phi)\rangle \neq 0$.
Since $\hat{K}(\phi)$ is diagonalizable,

$$\hat{K}(\phi)^n = \sum_j \lambda_j(\phi)^n |\lambda_j(\phi)\rangle\langle\lambda_j(\phi)|, \tag{A5}$$

and hence

$$\hat{\rho}_{A,n}^{(\mathrm{un})}(\phi) = \sum_{i,j} \lambda_i(\phi)^n \lambda_j(\phi)^{*n} c_{ij}(\phi) |\lambda_i(\phi)\rangle\langle\lambda_j(\phi)|, \tag{A6}$$

with $c_{ij}(\phi) = \langle\lambda_i(\phi)|\hat{\rho}_{A,0}|\lambda_j(\phi)\rangle$.
For $\phi < \phi_c$, the term with $|\lambda_1(\phi)|$ dominates as $n \to \infty$, leading to

$$\hat{\rho}_{A,\infty}(\phi) = \frac{|\lambda_1(\phi)\rangle\langle\lambda_1(\phi)|}{\langle\lambda_1(\phi)|\lambda_1(\phi)\rangle}, \tag{A7}$$

and, similarly for $\phi > \phi_c$, the dominant contribution comes from $\lambda_2(\phi)$.
Because the limiting projectors on either side of ϕ_c differ, the long-time meter state exhibits a discontinuity at ϕ_c, which directly transfers to the expectation values of observables.

[1] Yakir Aharonov, David Z Albert, and Lev Vaidman. How the result of a measurement of a component of the spin of a spin-1/2 particle can turn out to be 100. Physical review letters, 60(14):1351, 1988.

[2] Yakir Aharonov, Alonso Botero, Sandu Popescu, Benni Reznik, and Jeff Tollaksen. Revisiting hardy's paradox: counterfactual statements, real measurements, entanglement and weak values. Physics Letters A, 301(3-4):130–138, 2002.

[3] A Matzkin. Observing trajectories with weak measurements in quantum systems in the semiclassical regime. Physical review letters, 109(15):150407, 2012.

[4] Justin Dressel. Weak values as interference phenomena. Physical Review A, 91(3):032116, 2015.

[5] Lorena Ballesteros Ferraz, Dominique L Lambert, and Yves Caudano. Geometrical interpretation of the argument of weak values of general observables in n-level quantum systems. Quantum Science and Technology, 7(4):045028, 2022.

[6] Lorena Ballesteros Ferraz, Riccardo Muolo, Yves Caudano, and Timoteo Carletti. Revisiting weak values through non-normality. Journal of Physics A: Mathematical and Theoretical, 56(47):475303, 2023.

[7] Lorena Ballesteros Ferraz, Dominique Lambert, and Yves Caudano. Exploring weak value arguments and bargmann invariants in n-level quantum systems through the majorana symmetric representation. Journal of Physics A: Mathematical and Theoretical, 58(20):205303, 2025.

[8] Andrew N Jordan, Julián Martínez-Rincón, and John C Howell. Technical advantages for weak-value amplification: when less is more. Physical Review X, 4(1):011031, 2014.

[9] P Ben Dixon, David J Starling, Andrew N Jordan, and John C Howell. Ultrasensitive beam deflection measurement via interferometric weak value amplification. Physical review letters, 102(17):173601, 2009.

[10] Lan Luo, Xiaodong Qiu, Linguo Xie, Xiong Liu, Zhaoxue Li, Zhiyou Zhang, and Jinglei Du. Precision improvement of surface plasmon resonance sensors based on weak-value amplification. Optics Express, 25(18):21107–21114, 2017.

[11] Lorena Ballesteros Ferraz, John Martin, and Yves Caudano. On the relevance of weak measurements in dissipative quantum systems. Quantum Science and Technology, 9(3):035029, 2024.

[12] David RM Arvidsson-Shukur, William F Braasch Jr, Stephan De Bievre, Justin Dressel, Andrew N Jordan, Christopher Langrenez, Matteo Lostaglio, Jeff S Lundeen, and Nicole Yunger Halpern. Properties and applications of the kirkwood–dirac distribution. New Journal of Physics, 26(12):121201, 2024.

[13] Matthew F Pusey. Anomalous weak values are proofs of contextuality. Physical review letters, 113(20):200401, 2014.

[14] Ravi Kunjwal, Matteo Lostaglio, and Matthew F Pusey. Anomalous weak values and contextuality: Robustness, tightness, and imaginary parts. Physical Review A, 100(4):042116, 2019.

[15] Subir Sachdev. Quantum phase transitions. Physics world, 12(4):33, 1999.

[16] John A. Hertz. Quantum critical phenomena. Phys. Rev. B, 14, 1165:1165, 1976.

[17] AJ Millis. Effect of a nonzero temperature on quantum critical points in itinerant fermion systems. Physical Review B, 48(10):7183, 1993.

[18] Matthias Vojta. Quantum phase transitions. Reports on Progress in Physics, 66(12):2069, 2003.

[19] Markus Heyl, Anatoli Polkovnikov, and Stefan Kehrein. Dynamical quantum phase transitions in the transverse-field ising model. Physical review letters, 110(13):135704, 2013.

[20] Bojan Žunkovič, Alessandro Silva, and Michele Fabrizio. Dynamical phase transitions and loschmidt echo in the infinite-range xy model. Philosophical Transactions of the Royal Society A: Mathematical, Physical and Engineering Sciences, 374(2069):20150160, 2016.

[21] Stefano De Nicola, Alexios A Michailidis, and Maksym Serbyn. Entanglement view of dynamical quantum phase transitions. Physical Review Letters, 126(4):040602, 2021.

[22] Kohei Kawabata, Tokiro Numasawa, and Shinsei Ryu. Entanglement phase transition induced by the non-hermitian skin effect. Physical Review X, 13(2):021007, 2023.

[23] AA Zvyagin. Dynamical quantum phase transitions. Low Temperature Physics, 42(11):971–994, 2016.

[24] P Jurcevic, H Shen, P Hauke, C Maier, T Brydges, C Hempel, BP Lanyon, Markus Heyl, R Blatt, and CF Roos. Direct observation of dynamical quantum phase transitions in an interacting many-body system. Physical review letters, 119(8):080501, 2017.

[25] Brian Skinner, Jonathan Ruhman, and Adam Nahum. Measurement-induced phase transitions in the dynamics of entanglement. Physical Review X, 9(3):031009, 2019.

[26] Maxwell Block, Yimu Bao, Soonwon Choi, Ehud Altman, and Norman Y Yao. Measurement-induced transition in long-range interacting quantum circuits. Physical Review Letters, 128(1):010604, 2022.

[27] Yaodong Li, Yijian Zou, Paolo Glorioso, Ehud Altman, and Matthew PA Fisher. Cross entropy benchmark for measurement-induced phase transitions. Physical Review Letters, 130(22):220404, 2023.

[28] Crystal Noel, Pradeep Niroula, Daiwei Zhu, Andrew Risinger, Laird Egan, Debopriyo Biswas, Marko Cetina, Alexey V Gorshkov, Michael J Gullans, David A Huse, et al. Measurement-induced quantum phases realized in a trapped-ion quantum computer. Nature Physics, 18(7):760–764, 2022.

[29] Jin Ming Koh, Shi-Ning Sun, Mario Motta, and Austin J Minnich. Measurement-induced entanglement phase transition on a superconducting quantum processor with mid-circuit readout. Nature Physics, 19(9):1314–1319, 2023.

[30] Ricardo Puebla. Finite-component dynamical quantum phase transitions. Physical Review B, 102(22):220302, 2020.

[31] Ryusuke Hamazaki. Exceptional dynamical quantum phase transitions in periodically driven systems. Nature communications, 12(1):5108, 2021.

[32] Grazia Di Bello, Andrea Ponticelli, Fabrizio Pavan, Vittorio Cataudella, Giulio De Filippis, Antonio de Candia, and Carmine Antonio Perroni. Environment induced dynamical quantum phase transitions in two-qubit rabi model. Communications Physics, 7(1):364, 2024.

[33] Michel Bauer and Denis Bernard. Convergence of repeated quantum nondemolition measurements and wave function collapse. Phys. Rev. A, 84:044103, 2011.

[34] Michel Bauer and Denis Bernard. Repeated quantum non-demolition measurements: Convergence and continuous time limit. Annales Henri Poincaré, 13:1799–1821, 2012.

[35] M. Szyniszewski, A. Romito, and H. Schomerus. Entanglement transition from variable-strength weak measurements. Phys. Rev. B, 100:064204, 2019.

[36] Vimal Dubey, C. Bernardin, and Abhishek Dhar. Quantum dynamics under continuous projective measurements: Non-hermitian description and phase transitions. Phys. Rev. A, 103:032221, 2021.

[37] Guillaume Roux and et al. Partial wavefunction collapse under repeated weak measurement of a non-conserved observable. arXiv preprint, 2024.

[38] Martin Niss. History of the lenz-ising model 1920–1950: from ferromagnetic to cooperative phenomena. Archive for history of exact sciences, 59(3):267–318, 2005.

[39] Michael Kiometzis, Hagen Kleinert, and Adriaan MJ Schakel. Critical exponents of the superconducting phase transition. Physical review letters, 73(14):1975, 1994.

[40] Igor Poboiko, Igor V Gornyi, and Alexander D Mirlin. Measurement-induced phase transition for free fermions above one dimension. Physical Review Letters, 132(11):110403, 2024.

[41] Jacek Dziarmaga. Dynamics of a quantum phase transition and relaxation to a steady state. Advances in Physics, 59(6):1063–1189, 2010.

[42] Jan-Hendrik Prinz, Hao Wu, Marco Sarich, Bettina Keller, Martin Senne, Martin Held, John D Chodera, Christof Schütte, and Frank Noé. Markov models of molecular kinetics: Generation and validation. The Journal of chemical physics, 134(17), 2011.

[43] David A Levin and Yuval Peres. Markov chains and mixing times, volume 107. American Mathematical Soc., 2017.